Frequency-degenerate nonlinear light scattering in low-symmetry crystals

Alexandr Shumelyuk,[1,*] Alexandr Volkov,[1] Andreas Selinger,[2] Mirco Imlau,[2] and Serguey Odoulov[1]

[1]*Institute of Physics, National Academy of Sciences, 03 650 Kyiv, Ukraine*
[2]*Fachbereich Physik, Universität Osnabrück, Barbarastrasse 7, 49076 Osnabrück, Germany*
**Corresponding author: shumeluk@iop.kiev.ua*

Received August 1, 2007; revised November 20, 2007; accepted November 22, 2007;
posted December 4, 2007 (Doc. ID 85666); published January 9, 2008

A considerable distinction of light-induced scattering in optically biaxial crystals comes from the fact that the principal axes of the optical indicatrix do not coincide with the crystallographic directions. The study of photorefractive scattering in $Sn_2P_2S_6$ (monoclinic symmetry) revealed the particular requirements as to light polarization for excitation of parametric scattering and the polarization inhomogeneity of wide-angle scattering. © 2008 Optical Society of America

OCIS codes: 190.5330, 160.2260.

Tin hypothiodiphosphate ($Sn_2P_2S_6$,SPS) is known as a photorefractive material with fast (microsecond range) temporal response and high (about 10 cm^{-1}) two-beam-coupling gain (see, e.g., the review chapter [1]). The light-induced space charge develops via diffusion-mediated transport (possibly, via charge hopping in the near infrared [2]), thus explaining the pronounced two-beam coupling.

At room temperature SPS belongs to the symmetry class m, the y axis being normal to the mirror plane and the x and z axis making an angle of 91.15° [3], i.e., an angle only slightly different from 90°. The electro-optic (Pockels) tensor of SPS possesses 10 nonvanishing components, the largest known being $\simeq$174 pm/V [4]. A standard geometry for index grating recording involves two beams that impinge upon a z-cut sample in a plane normal to the y axis and polarized along the x axis [1]. For z-cut SPS samples a strong wide-angle light-induced scattering was reported [5], similar to the beam fanning in crystals with the diffusion transport [6].

Apart from polarization-isotropic scattering, the structure of Pockels tensor for these crystals allows one to expect various kinds of anisotropic scattering with polarization orthogonal to that of the incident beam [7]. Surprisingly, for a material with a high gain, to our knowledge such a scattering has never been mentioned in publications about SPS and most probably has not been observed at all.

This Letter describes the observation of several qualitatively new features of photorefractive scattering in optically biaxial crystals such as SPS. As distinct from what is known for birefringent crystals with one optical axis, it was found that (1) the polarization of the wide-angle scattering is not uniform but depends on the scattering angle, (2) to observe conical parametric scattering the polarization of the incident beam should be adjusted not in the direction where the largest electro-optic constant defines the gain factor but according to the orientation of the optical indicatrix, and (3) for hyperbolic scattering the foci are not located along crystallographic axes.

Several SPS crystals grown in the University of Uzhgorod, Ukraine, were studied. The samples were cut along the crystallographic axes; they typically are a few millimeters thick and have optically finished faces. An unexpanded beam of an Ar^+/Kr^+ laser entered the sample through one face while the scattering pattern was observed on a screen behind the sample (Fig. 1). In such a way only those patterns were analyzed that are due to the recording of transmission index gratings [7].

For z-cut and x-cut samples the wide-angle scattering is aligned along the positive direction of the x and z axes, respectively. The scattering is strong in z-cut samples and comparably weak in x-cut samples. The scattered waves polarization is the same as that of the incident wave.

A rich variety of scattering processes is found for y-cut samples. If the incident light is polarized along the x axis (polarization unit vector $\mathbf{e}$ has the components {1,0,0}) or along the z axis ($\mathbf{e}$={0,0,1}) bright hyperbolic lines appear, centered to the y direction. Figure 2a shows an example for the incident beam tilted 20° with respect to the y axis in the xz plane.

If the polarization of the incident beam is rotated roughly to ±45°, the wide-angle scattering becomes dominant. Figure 2b shows a scattering pattern for the incident light with $\mathbf{e}$={1,0,1}. For orthogonally polarized incident light, with $\mathbf{e}$={1,0,−1}, a fraction of the polarization-anisotropic ring can be seen in addition to wide-angle scattering (Fig. 2c). The hyperbolic patterns do not appear in the two last cases.

We attribute the wide-angle scattering to amplification of optical noise via direct coupling with the incident wave. In contrast, hyperbolic and ring structures are assigned to parametric mixing of four and three copropagating beams, respectively.

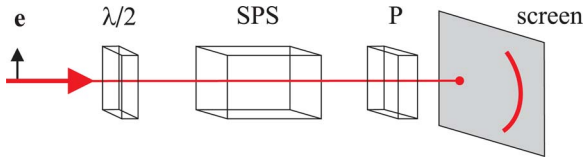

Fig. 1. (Color online) Setup for the observation and study of the scattering patterns. SPS, photorefractive sample; λ/2, phase retarder; P, polarizer.

0146-9592/08/020150-3/$15.00

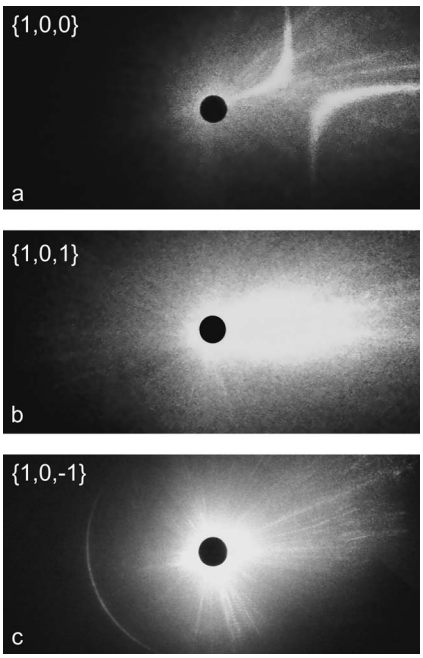

Fig. 2. Scattering patterns in y-cut SPS sample for different polarizations of the incident light beam. No polarizer is put between the sample and screen for patterns a and b. For pattern c the intensity of the wide-angle scattering is strongly suppressed. The incident light polarization is indicated in each frame.

In spite of the apparent similarity of the scattering pattern of Fig. 2b to classical beam fanning in $BaTiO_3$ [6] there exists an important distinction between the two cases: the polarization of fanning in $BaTiO_3$ is uniform, the same as that of the incident wave. With an appropriately adjusted polarizer the intensity can be reduced to zero throughout the whole scattering lobe. The scattering shown in Fig. 2b, on the contrary, is not uniform in its polarization: when rotating a polarizer one can move a dark fringe along the scattering lobe. The deviation of polarization of a particular component in scattered light from the polarization of incident light increases with increasing angle between the incident and scattered light.

The properties of the parametric scattering are unusual, too. Nontrivial conditions of excitation of a ring scattering have already been described. For hyperbolic scattering the foci appear on the bisector of the axes x and z, as distinct from, e.g., the scattering in $LiNbO_3$:Fe, where the foci are located along the z axis [7].

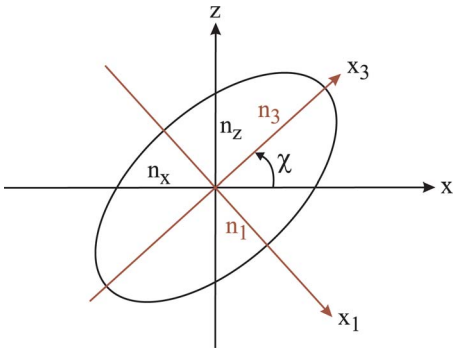

Fig. 3. (Color online) Optical indicatrix in the xz plane. The angle between the x axis and the longest axis of the ellipse is $\chi = 43.3°$ for $\lambda = 633$ nm at room temperature [8].

To explain specific manifestations of the light-induced scattering in SPS one needs to consider the optical indicatrix of this biaxial crystal. The ellipsoid of the refractive indices lies in the mirror plane; n_1 and n_3 axes of the ellipsoid are in the xz plane, while the n_2 axis is normal to this plane. Figure 3 represents a sketch of the indicatrix in the xz plane with the emphasized difference in n_1 and n_3 indices.

At room temperature the long axis of the indicatrix for 633 nm light is aligned roughly along the bisector of the z and x axes (one can find precise data on temperature and wavelength dependences of the indicatrix parameters in [8]). From Fig. 3 we see that the eigenwaves of y-cut SPS have the polarization unit vectors close to $\mathbf{e}_1 \approx \{1, 0, -1\}$ and $\mathbf{e}_3 \approx \{1, 0, 1\}$. At the same time, for x-cut or z-cut SPS the eigenwaves are polarized along the crystallographic axes, for example, $\mathbf{e}_2 = \{0, 1, 0\}$. This means that when changing the direction of the light-beam propagation from the z to the y axes one will see a gradual rotation of the polarizations of two eigenwaves. We calculate the eigenwave polarization angle ν versus beam incident angle β in the xy plane (see Fig. 4) with only one assumption, that the n_2 axis of the optical indicatrix of the crystal of point group m is aligned along the y axis:

$$\nu = \frac{1}{2}\tan^{-1}\left[\frac{(n_1^{-2}\sin 2\chi - n_3^{-2}\sin 2\chi)\sin\beta}{(n_1^{-2}\sin^2\chi + n_3^{-2}\cos^2\chi)\sin^2\beta + n_2^{-2}\cos^2\beta - n_1^{-2}\cos^2\chi - n_3^{-2}\sin^2\chi}\right]. \quad (1)$$

The dependence shown in Fig. 4 allows us to explain the spatial inhomogeneity of the beam fanning in y-cut SPS. The most strongly amplified scattering waves are those for which the polarization does not change with propagation, i.e., the scattering waves with eigenpolarization. These waves form, together with the incident wave, the fringes with the contrast that does not oscillate in space. Consequently, the space-charge field produced by these fringes is high everywhere in the crystal bulk, and relevant scattered waves are amplified stronger than others.

For scattered components that are not eigenwaves of the sample the polarization state changes with propagation distance. At certain distances the slab of

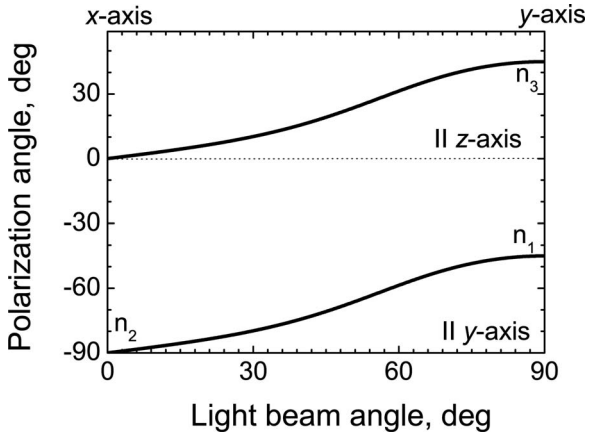

Fig. 4. Polarization angle of the eigenwaves versus beam propagation angle in the xy plane. n_1, n_2, and n_3 mark conditions at which the refractive index takes its principal values.

SPS acts as a lambda half-phase retarder that rotates the linear polarization to 90°. The fringe contrast at these distances drops to zero, and no space-charge field develops. It is obvious that such a scattered wave is amplified much less than that with eigenpolarization. As the polarization of the eigenwave depends on the direction of its propagation (Fig. 4) the polarization of the wide-angle scattering (Fig. 2b) follows this dependence.

The unusual orientation of the optical indicatrix in SPS, which is aligned along the bisector of the x and z axes, defines the position of the hyperbolic scattering foci that are located on the longest axis of the index ellipsoid. To excite a hyperbolic scattering a mixture of two eigenwaves needs to propagate inside the crystal so that the wave vectors $\mathbf{k}$ obey the phase-matching condition

$$\mathbf{k}_{\mathrm{inc}}^{(3)} - \mathbf{k}_{\mathrm{inc}}^{(1)} = \mathbf{k}_{\mathrm{scat}}^{(3)} - \mathbf{k}_{\mathrm{scat}}^{(1)}. \quad (2)$$

Here, the upper indices mark eigenpolarizations, and lower indices mark the incident (inc) and scattered (scat) waves. Thus the axes of the index ellipse shown in Fig. 3 define the symmetry axes for the hyperbolic scattering pattern. The fact that hyperbolic scattering does not appear when only one of two eigenpolarizations is present in the incident beam also follows directly from Eq. (2).

As opposite to hyperbolic scattering, the anisotropic ring scattering comes from only one wave with eigenpolarization, namely, from that with the smallest index n_1. The relevant phase-matching condition reads as

$$\mathbf{k}_{\mathrm{inc}}^{(1)} - \mathbf{k}_{\mathrm{scat}}^{(1)} = \mathbf{k}_{\mathrm{scat}}^{(3)} - \mathbf{k}_{\mathrm{inc}}^{(1)}. \quad (3)$$

The best condition for observation of a ring, therefore, is to illuminate the sample with the wave that contains only one polarization n_1, which is in full agreement with our observations.

The scattering angles for parametric processes such as those described by Eq. (3) are very sensitive to the difference in the refraction indices of eigenwaves and vary with the laser wavelength. This was verified experimentally: the apex angle $\theta \approx 32°$ is measured at $\lambda = 568$ nm as compared with $\theta \approx 25°$ at $\lambda = 647$ nm. These values are in good agreement with the estimate that is done with the known data on the index dispersion of SPS [8] from the relationship that follows directly from Eq. (3) [see [7] for the details of the derivation of Eq. (4)]:

$$\theta \approx \sqrt{(n_3 + n_1)(n_3 - n_1)/2}. \quad (4)$$

To conclude, we observed, for the first time to our knowledge, the anisotropic conical scattering in $Sn_2P_2S_6$ and found and explained particular features of several kinds of photorefractive scattering in this material, which are related to its low symmetry. It should be emphasized that the observed nonlinear conical scattering has nothing in common with the linear effect of anomalous conical refraction typical for optically biaxial crystals [9]: the latter can be oberved only when the light wave is propagating along one of the two optical axes of the crystal, while the conical scattering that we observe can be excited over a wide range of angles, even 50° away from the optical axis.

The authors thank A. Grabar and I. Stoyka for SPS samples and E. Krätzig for helpful discussions. Financial support from Deutsche Forschungsgemeinschaft (GRK 695, IM 37/2-2) and Alexander von Humboldt Stiftung (research award for S. Odoulov) is gratefully acknowledged.

References

1. A. Grabar, M. Jazbinšek, A. Shumelyuk, Yu. M. Vysochanskii, G. Montemezzani, and P. Günter, in *Photorefractive Materials and Their Applications 2*, P. Günter and J.-P. Huignard, eds. (Springer-Verlag, 2007), pp. 327–362.
2. S. Odoulov, A. Shumelyuk, U. Hellwig, R. Rupp, A. Grabar, and I. Stoyka, J. Opt. Soc. Am. B **13**, 2352 (1996).
3. G. Dittmar and H. Schafer, Z. Naturforsch. B **29**, 312 (1974).
4. D. Haertle, G. Caimi, A. Haldi, G. Montemezzani, A. Grabar, I. Stoyka, and Yu. Vysochanskii, Opt. Commun. **215**, 333 (2002).
5. I. Kedyk, A. Grabar, M. Gurzan, and Yu. Vysochanskii, Visngk Lviv Natl. Univ. Phys. Ser. Phys. **36**, 174 (2003).
6. J. Feinberg, J. Opt. Soc. Am. **72**, 46 (1982).
7. B. I. Sturman, S. G. Odoulov, and M. Yu. Goul'kov, Phys. Rep. **275**, 197 (1996).
8. D. Haertle, A. Guarino, J. Hajfler, G. Montemezzani, and P. Günter, Opt. Express **13**, 2046 (2005).
9. A. Yariv and P. Yeh, *Optical Waves in Crystals* (Wiley, 1984).